Infiltrative glioma detected by Fast Field Cycling NMR: a Nuclear Magnetic Resonance technology of low and variable magnetic fields

Manuel Petit, Sandra Pierre, Maxime Leclercq, and **Hana Lahrech**
BrainTech Lab - INSERM U1025 – Grenoble, France

Purpose

Fast Field Cycling Nuclear Magnetic Resonance (FFC-NMR), which measures relaxation times T_1 at different magnetic fields (T_1-dispersion profiles or R_1-dispersion profiles where $R_1 = 1/T_1$) in low regime (here from 0.1mT to 1T) is especially used in physics and chemistry to characterize the molecular dynamics of the materials. Here our aim is to highlight the role of FFC-NMR in detecting glioma cell infiltration in brain tissue. For the first time, we use this technology in neuro-oncology to assess its feasibility to discriminate between solid and infiltrative tumours. Using mathematical models, we aim to describe T_1-dispersion profiles and to find how the numerical parameters derived either from T_1-dispersion profiles or from quadrupolar peaks that result from the nuclei interactions of the nitrogen of proteins and the hydrogen of water (QPs of ^{14}N-^{1}H nuclei coupling) could be exploited as biomarkers for glioma characterization.

Subjects and Methods

Three glioma mouse models were studied: the U87, a standard model of solid glioma, the glioma Glio6 and the Glio96 mouse models of tumour cell migration/invasion, both derived from human stem cells and developed in our laboratory. The Glio6 was recently validated[1] while the Glio96 is still under study. After the tumour growth controlled in a MRI follow-up, brains (n=18 for each model) were removed, and regions of U87 solid glioma and of Glio6 and Glio96 glioma cell infiltration were extracted (30 to 210mg weight) and stored at -80°C. Histology (Hematoxylin/Eosin (HE) and Hematoxylin/Eosin/Safran (HES)) were used to confirm the nature of the sample.

T_1-dispersion profiles were acquired on the FFC-NMR relaxometer, a Stelar machine localized at the Grenoble CEA and analysed using the power mathematical model[2] of the [Eq.1], to describe the background of T_1-dispersion profiles with two regimes, at low and high magnetic fields. A is the amplitude at the origin, β_L and β_H the exponents at low and high fields known to relate to molecular dynamics[2] and ν_0^d is the frequency at the discontinuity. [Eq.2] is the model that describes the QPs[3] where A_{QP} is their amplitude, ω_Q and η parameters set the peak frequencies, τ is the rotational correlation time and θ and φ are the spherical coordinates of the quadrupole vector. Three parameters (A, β_L, A_{QP}) were then selected using the non-parametric Kruskal–Wallis test which investigate the distribution differences between the classes and thus their separability. All the analysis was achieved using the software MATLAB©.

$$R_1(B_0) = \begin{cases} A(\gamma B_0)^{\beta_L}, & \gamma B_0 < \nu_0^d \\ A(\nu_0^d)^{\beta_L-\beta_H}(\gamma B_0)^{\beta_H}, & \nu_0^d \le \gamma B_0 \end{cases} \quad with\ \gamma = \gamma/2\pi \qquad \text{[Eq.1]}$$

$$R_{1Q}(\omega_0) = A_{QP} \sum_{\lambda=X,Y,Z} \left(\frac{1}{3} + u_\lambda^2\right)\left(\frac{\tau}{1+(\omega_0-\omega_\lambda)^2\tau^2} + \frac{\tau}{1+(\omega_0+\omega_\lambda)^2\tau^2}\right) with \begin{cases} \omega_X = \omega_Q(3+\eta)\ ;\ u_X = \sin(\theta)\cos(\varphi) \\ \omega_Y = \omega_Q(3-\eta)\ ;\ u_Y = \sin(\theta)\sin(\varphi) \\ \omega_Z = 2\omega_Q\eta\ ;\ u_Z = \cos(\theta) \end{cases} \qquad \text{[Eq.2]}$$

Result

Fig.1 presents the mean R_1-dispersion profiles of Glio6, Glio96 and U87 glioma. The curves showed an excellent power-law shapes (R>0.98) indicating dominant relaxation by protein matrix[2]. In all curves the signal of QPs was present and accurately fitted to Eq.2. Glio6 and Glio96 curves were well separated from U87 glioma.

In Fig.2, we see that the parameters A, amplitude and β_L, low-field slope derived from the power model and the QPs amplitude A_{QP} clearly discriminate solid tumour class from infiltrative glioma cells. The parameter A indicated a net difference in T_1 relaxation while the component β_L showed molecular dynamics in its frequency range. The amplitude of the QP is known to be sensitive to immobile protein molecules[4], a feature completely invisible to conventional NMR/MRI that can also be exploited for additional molecular information. In Fig.2 we can see that the power offset A and the low-field slope β_L evaluated by the Kruskal–Wallis test, are the two most discriminant parameters.

Conclusion/Discussion

Peritumoural regions invaded by infiltrative glioma cells are not adequately and sufficiently early diagnosed by MRI or any current medical imaging method. This study highlights the great interest of FFC-NMR methods, a new technology in neuro-oncology and in cancer research to exploit molecular dynamics that are not visible by any other methods.

These results were also observed in human resection[5] and highlight the interest to develop FFC-MRI for clinical investigations, an European H2020 project (IDentIFY: Improving Diagnosis by Fast Field Cycling MRI) which is under progress.

References:

[1]Gimenez U, Perles-Barbacaru AT, Apaix F, El-Attifi M, Pernel-Galley K, Berger F, Lahrech H, Microscopic DTI accurately identifies early glioma cell migration: correlation with multimodal imaging in glioma stem model, NMR in Biom 29:1553-1562 (2016)

[2]Kimmich R, Winter F, Nusser W, Sspohn KH, Interactions and Fluctuations Deduced from Proton Field-Cycling Relaxation Spectroscopy of Polypeptides, DNA, Muscles, and Algae, JMR 68: 263-282 (1986)

[3]Fries PH, Belorizky E, Simple expressions of the nuclear relaxation rate enhancement due to quadrupole nuclei in slowly tumbling molecules, Journal of Chemical Physics 143 (2015)

[4]Kimmich, Rainer & Anoardo, Esteban, Field-cycling NMR relaxometry. Progress in Nuclear Magnetic Resonance Spectroscopy, 44. 257-320 (2004).

[5]Broche LM , Huang Y , Pierre S, Berger F , Lurie D J , Fries PF , and Lahrech H, Fast Field-Cycling NMR of human glioma resections: characterization of heterogeneity, ISMRM Honolulu USA (2017)

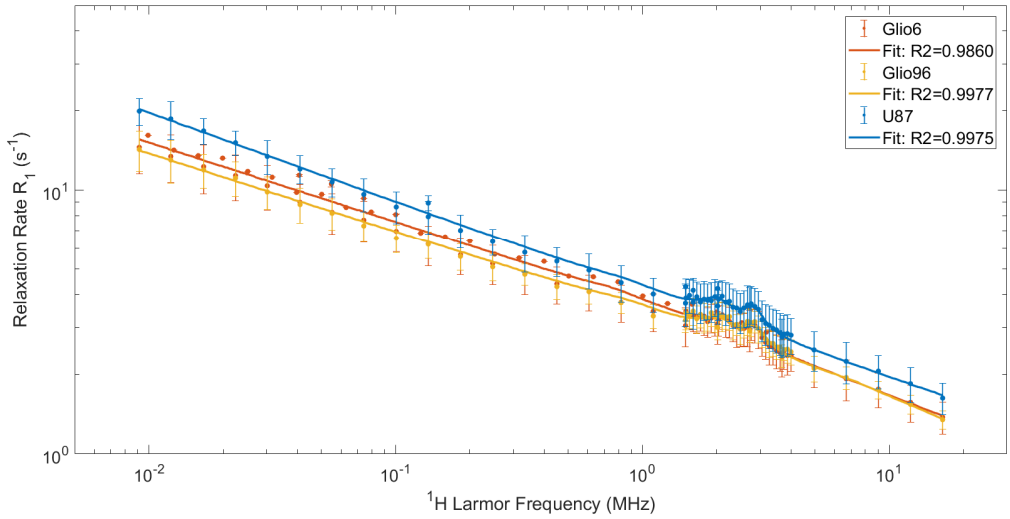

Fig. 1: Mean R_1-dispersion profiles (Relaxation rate $R_1=1/T_1$ versus ^{1}H Larmor frequency $\nu_0=\gamma/2\pi B_0^E$) of U87, Glio6 and Glio96. The errorbars correspond to one standard deviation. The fits (continuous lines) were achieved using both the models presented in Eq. 1 and 2.

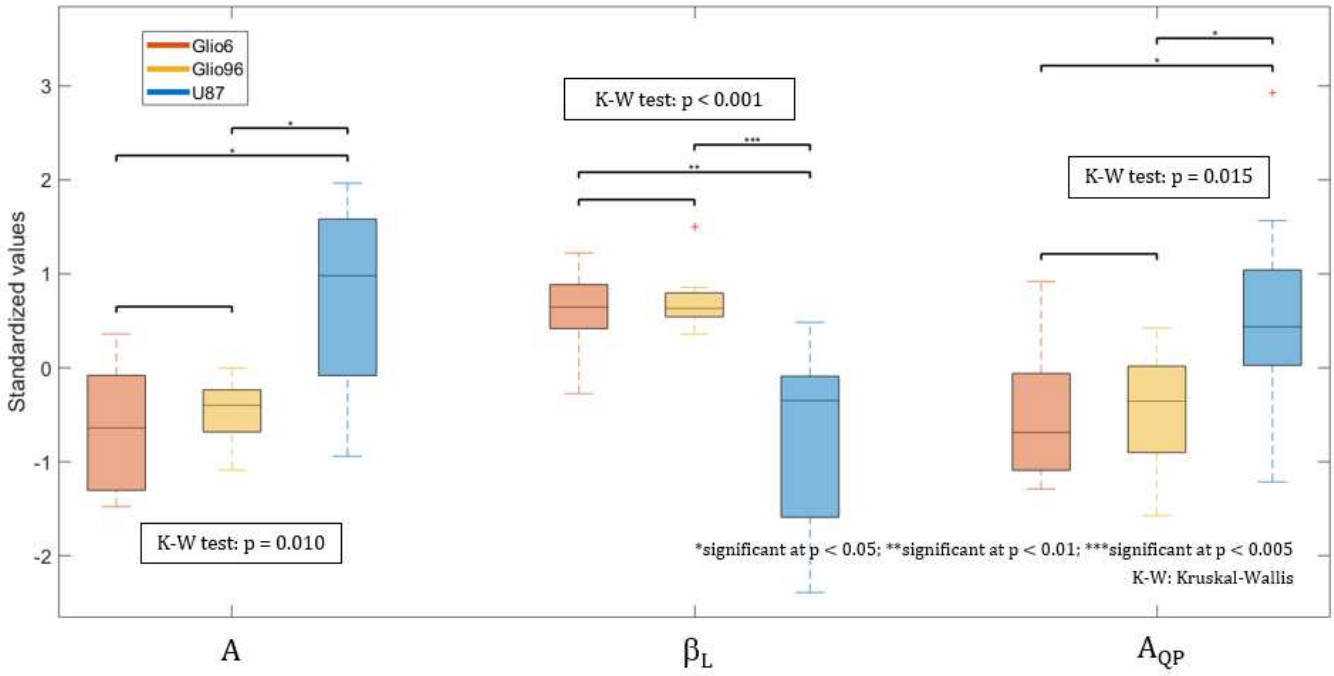

Fig. 2: Boxplot of the three selected mathematical parameters. On each box, the central mark indicates the median, and the bottom and top edges of the box indicate the 25th and 75th percentiles, respectively. The whiskers, bottom and top, indicate the 9th and 91th percentiles, respectively. The outliers are plotted using the '+' symbol. The non-parametric Wilcoxon rank sum test was applied to control the null hypothesis that data have equal medians. For visual purposes only standardized values are displayed.